Prediction on the effective thermal conductivity of highly compacted GMZ01 bentonite based on intermingled fractal units theory

Z.R. Liu
Department of Geotechnical Engineering, Tongji University, Shanghai 200092, China

Y.J. Cui
Ecole Nationale des Ponts et Chaussées, Paris, France

W.M. Ye
Key Laboratory of Geotechnical and Underground Engineering of Ministry of Education, Tongji University, Shanghai 200092, China

ABSTRACT: Gaomiaozi (GMZ) bentonite has been selected as the possible materials for the construction of engineered barrier in geological repository for high-level radioactive waste (HLW) disposal in China. As one of the key parameters used in the performance assessment of the HLW repository, the thermal conductivity of GMZ01 bentonite was investigated in this study based on the intermingled fractal units (IFU) theory. A prediction model for effective thermal conductivity (ETC) was proposed with consideration of microstructure characteristics. According to the pore size distribution obtained from MIP test, the microstructure of GMZ01 bentonite was firstly geometrically simulated by means of numerous intermingled fractal units (IFU). Then, the ETC was calculated via series-parallel electrical analogy equivalently converted from the IFU model. Results show that the calculated values agree well with the experimental data. The results under different conditions also show that the ETC of GMZ01 bentonite was largely governed by its dry density and water content. This IFU model constitutes a helpful tool for further numerical modeling of the thermo-hydro-mechanical (THM) behavior of GMZ01 bentonite.

1 INTRODUCTION

In most countries involved in nuclear waste disposal, bentonite has been selected as one of the candidate buffer/backfill materials in the high-level radioactive waste (HLW) repository due to its low permeability, high swelling and favorable radionuclide retardation capacities. For instance, in the conceptual repository of KBS-3 (Laine and Karttunen 2010), compacted bentonite or bentonite-based materials are used to fill the annular space between the waste canister and host rock, being expected to delay the radionuclide transfer to the lithosphere and biosphere, and to contribute to the mechanical stability of the disposal tunnel. After emplacement, the compacted bentonite buffer will be subjected to a relatively high temperature up to 150℃ generated by the long-lasting decay heat released by the wastes, and conduct it to the host rock (Johnson et al. 2002). This heat conduction process is mainly controlled by the thermal conductivity of the bentonite buffer. With a too low thermal conductivity, the accumulated heat may lead to unfavorable mineralogical alterations (e.g., illitization, silicification, etc.) and hydro-mechanical behavior deterioration (e.g., embrittlement and water retention reduction) of the bentonite, and consequently compromising its engineering barrier performance (Pusch et al. 2003; Wersin et al. 2007; Dueck and Börgesson 2015; Wan et al. 2015). Therefore, it is of paramount importance to study the thermal conductivity of compacted bentonite.

The thermal conductivity of various compacted bentonite or bentonite-based materials has been measured via either transient plane source method or transient line source method. Empirical or statistical models as functions of physical parameters (e.g., water content, dry density, porosity, the volumetric fraction of air) were correspondingly proposed for predictions (Liu et al. 2007; Tang et al. 2008; Ye et al. 2010; Cho et al. 2011). These models were phenomenological in essence and failed in directly relating the thermal conductivity to the soil microstructure. Recently, some analytical models have been developed, among them, a series-parallel structural model and an effective thermal conductivity (ETC) model (Chen et al. 2014; Chen et al. 2015). But these two models either ignored the microstructure of compacted bentonites or included a relatively complicated homogenization approach. More details can be found in recent reviews by Barry-Macaulay et al. (2015) and Dong et al. (2015).

The present study aims at predicting the ETC of unsaturated compacted GMZ01 bentonite with a new IFU theory-based model, which was firstly proposed and applied by Atzeni et al. (2008). The model implies soil pore size distribution (PSD) curve and the known thermal conductivity of each phase of soil. A

comparison between the predicted and the measured results indicates the performance of the model.

2 FRACTAL THEORY AND ITS APPLICATION TO SOIL MICROSTRUCTURE

2.1 *Basic concepts*

Fractal, a term stemmed from Latin word fractus (broken/fractured), had been used to name a developed geometry by Mandelbrot (1967) - the exactly self-similar fractals are defined as a fractal set for which the Hausdorff-Besicovitch dimension strictly exceeds the topological dimensions. Many exactly self-similar fractals can be obtained by iterative method resulting in different fractal dimensions, which are indexes for characterizing fractal patterns or sets by quantifying their complexity as a ratio of the change in detail to the change in scale. Taking the well-known Sierpinski carpet as an example (Figure 1), it can be obtained by removing N_s squares from an initial square with N parts equally divided side, and then repeat this process in the residual $N^2 - N_s$ squares with the same procedure till a target figure. In this situation, the fractal dimension D_f can be calculated as:

$$D_f = \ln(N^2 - N_s)/\ln N \tag{1}$$

where N is the number of divisions of the side, N_s is the number of sub-cubes subtracted at each iteration. In Figure 1, $N = 3$ and $N_s = 1$. Thus, its fractal dimension $D_f = 1.893$. If the removed squares stand for pores, the porosity ϕ_i and pore diameter λ_i at i^{th} iteration can be respectively calculated as:

$$\phi_i = 1 - \left(\frac{N^2 - N_s}{N^2}\right)^{i+1} \tag{2}$$

and

$$\lambda_i = \frac{\lambda_0}{N^i} \tag{3}$$

where i is the iteration number, $i = 0,1,2\cdots$, and λ_0 is the initial pore diameter.

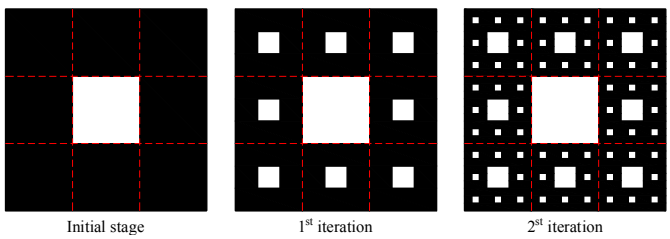

Figure 1. A typical Sierpinksi carpet geometry

However, almost all the fractal geometries in nature are not as exactly self-similar as Sierpinski carpet, but statistically self-similar. In the past three decades, a lot of studies revealed that soils are fractals statistically, and thus fractal theory can be applied (Xu et al. 1997; Perrier et al. 1999; Bartoli et al. 2010).

2.2 *The non-fractal feature of the pore size distribution of highly compacted bentonite*

Pfeifer and Avnir (1983) reported that the fractal pore structure is related to its fractal dimension by:

$$-\frac{\mathrm{d}V}{\mathrm{d}\lambda} \propto \lambda^{2-D_\mathrm{f}} \tag{4}$$

where V is the cumulative pore volume with pore diameter no smaller than λ.

This expression can be further rewritten as:

$$\log(-\frac{\mathrm{d}V}{\mathrm{d}\lambda}) \propto (2 - D_\mathrm{f})\log(\lambda) \tag{5}$$

Therefore, in a bi-log diagram of $-\mathrm{d}V/\mathrm{d}\lambda$ vs. λ obtained from mercury intrusion porosimetry (MIP), the gradient of its optimum linear fitting line equals $(2 - D_\mathrm{f})$, and in turn the fractal dimension D_f of the pore size distribution can be easily calculated. This method has been widely applied to account for the soil microscopic structure. For example, Xu (2004) analyzed the pore size distribution of a glacial till with a similar procedure, Pia and Sanna (2013a) fitted the bi-log PSD curves of insulating concrete and wooden aggregate respectively with a single line to show their fractal feature.

Nevertheless, some soils such as compacted bentonite usually present one or more peaks in their PSD curves (Figure 2), consequently their $\log(-\mathrm{d}V/\mathrm{d}\lambda)$ vs. $\log(\lambda)$ curves have to be piecewise fitted as two or more straight lines with different gradients (Figure 3). In this situation, only a few of the fitting lines can reproduce a canonical fractal dimension ($D_\mathrm{f} < 3$). Obviously, these kinds of PSD curves are non-fractal, and can hardly be analysed by conventional fractal iteration procedures.

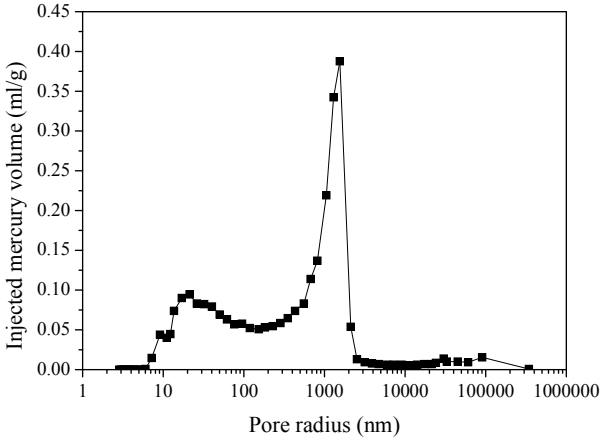

Figure 2. Pore size distribution curves of a GMZ01 compacted bentonite at 1.5 Mg/m^3. (Chen et al. 2016)

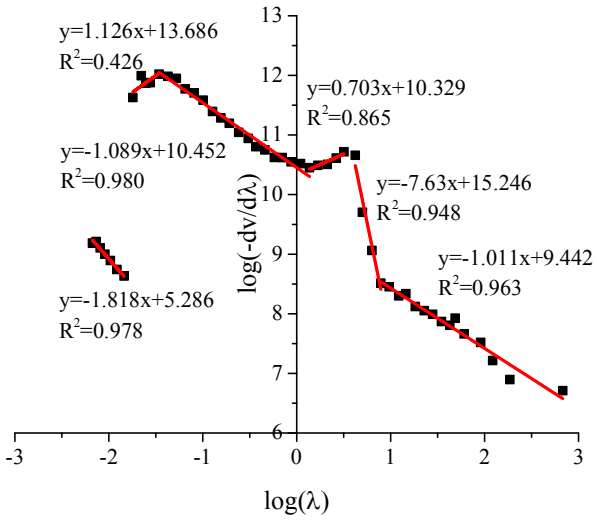

Figure 3. Log-log plot of the PSD curve and piecewise liner fitting lines of a GMZ01 compacted bentonite at 1.5 Mg/m^3, where λ in μm and V in μm^3.

This phenomenon, however, was commonly ignored in previous studies where the soil porosity was uncritically defined as fractal without taking the pore size distribution into consideration (Pia and Sanna 2013b).

3 THE IFU MODEL AND ELECTRICAL-THERMAL CONDUCTIVITY PATTERNS

In order to simulate the pore size distribution of either fractal or non-fractal, the intermingled fractal units (IFU) model developed by Atzeni at al. (2008) was adopted. In this model:

- the microstructure of soil was rebuilt with two or more Sierpinski type fractal units and a certain area of solid surface, and with strict correspondence to the real pore size distribution obtained from MIP test;
- each fractal unit was converted into electrical equivalent circuit, and the ETC k_{eff} was calculate by series and parallel combinations (Figure 4);
- the initial Sierpinski type fractal units were considered as part of the "solid" phase of the next stage of fractal iteration, with a k_s equivalent to k_{eff} calculated previously, i.e., the k_{eff} calculated in step n is inserted into step (n+1) as the new value of the conductivity of the "solid" phase.
- Finally, the k_{eff} of the integral IFU configuration was obtained by performing an area-weighted average on the whole fractal units and the filled solid surface. More details can be found in Pia and Sanna (2013a, 2013b, 2014a, 2014b).

Though innovative and effective, the number and type of FU in Pia and Sanna's work were established by trial and error without any certain patterns to follow. Moreover, the cases of soils in unsaturated state were excluded from their studies. The present study aims at refining these deficiencies for an application to highly compacted bentonite.

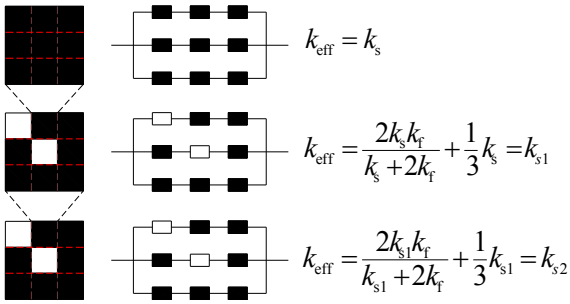

Figure 4. Fractal procedure and the electrical equivalent circuits, where k_s and k_f are the thermal conductivities of solid and fluid phases, respectively.

4 PREDICTION ON THE ETC OF HIGHLY COMPACTED GMZ01 BENTONITE

4.1 *IFU configuration and Electrical analogy*

As China's first candidate buffer material, GMZ01 bentonite is a montmorillonite dominant Na-bentonite with cation exchange capacity and plastic index as high as 77.30 meq /100 g and 275, respectively (Wen and Jintoku 2005). Among various properties, its thermal conductivity at different states has been experimentally studied by Liu et al. (2007) and Ye et al. (2010).

In the present study, firstly, 5 specimens with the same diameter (50 mm) and height (110 mm) were prepared by compaction. Their dry densities were 1.5 Mg/m^3, 1.7 Mg/m^3 and 1.9 Mg/m^3. Different water contents (i.e., 10.60%, 13.30%, 13.43%) were considered. Then, these specimens were subjected to thermal conductivity measurement using a commercial thermal properties analyzer, KD2 PRO. Detailed description of the measurement method can be found in Tang et al. (2008) and Ye et al. (2010). The test results are shown in Table 1.

Table 1. The initial conditions and measured thermal conductivity values of GMZ01 bentonite

Series	ρ_d (Mg/m^3)	w (%)	k (W/mK)
1	1.4	13.30	0.764
2	1.5	10.60	0.730
3	1.7	10.60	0.851
4	1.7	13.43	1.172
5	1.9	10.60	1.061

After the thermal conductivity measurement, small cubes of soil were taken from each specimen and freeze-dried for mercury intrusion porosimetry (MIP) tests to obtain their pore size distributions. The PSD curve of series 3 is plotted as black solid line in Figure 5, which covers a pore diameter range from about 10 nm to 357 000 nm.

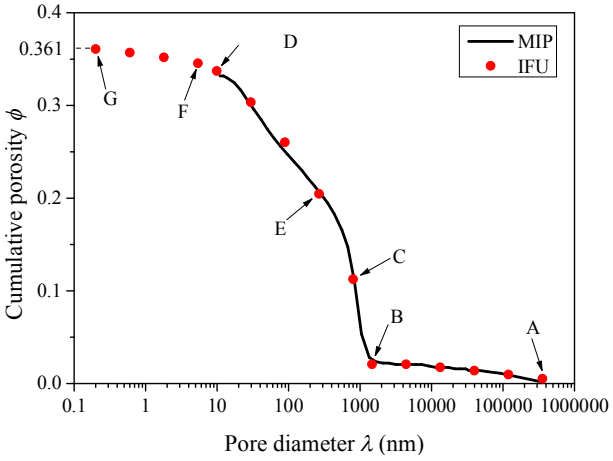

Figure 5. The pore size distribution curve from MIP test (solid line) and IFU model (dot) of Series 3 in Table 1.

Instead of trial and error method used by Pia and Sanna (2013a, 2013b, 2014a, 2014b), the IFU configuration with only three simple Sierpinski type fractal units (Figure 6) following a more definite and imitable procedure was developed, as follows.

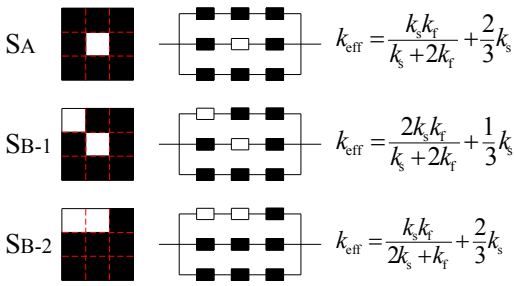

Figure 6. Sierpinski type fractal units used for IFU configuration and the electrical equivalent circuits.

1) Determining the pore diameter scope of the specimen from the PSD curve and calculating the total porosity according to:

$$\phi = 1 - \frac{\rho_d}{G_s \rho_w} \tag{6}$$

where ϕ is the porosity, ρ_d is the dry density (Mg/m^3), G_s is the specific gravity of solid phase, $G_s = 2.66$ (Wen and Jintoku 2005), ρ_w is the density of water (Mg/m^3). In the present case, the pore diameter scope was determined as about 10 nm to 357 000 nm, and the total porosity was calculated to be 0.361.

2) Determining the pore size scope for each fractal unit. Four characteristic points A, B, C and D (Figure 5, Table 2) were selected as the dividing point of the PSD curve and correspondingly at least 3 fractal units I, II, and III were required to simulate the curve.

Table 2. The characteristic points to divide the PSD curve.

Points	λ (nm)	ϕ	Characteristic
A	357000	0.005	The maximum pore size.
B	1469	0.021	Where the curve begin to increase sharply.
C	800	0.113	The "large pore" diameter.
D	10	0.337	The minimum pore size on the curve.
E	266.67	0.205	The sub-pore size of fractal unit II at 1th iteration.
F	5.4	0.345	The sub-pore size of fractal unit III at 1th iteration.
G	0.2	0.361	The minimum pore size as considered by Lloret and Villar (2007).

3) Simulating the PSD curve by IFU model. Three simple Sierpinski type fractal units (i.e. SA, SB-1 and SB-2, Figure 6) were chosen to build the IFU configuration which was consists of five parts: fractal unit I, II, III, IV, and the filled surface. Among them, fractal unit I was a 5-step iterated SA type Sierpinski carpet with a maximum pore size 357000 nm, while fractal units II, III, IV were SB-1 or SB-2 type Sierpinski carpet in equal probability (Table 3). The parameters of IFU model were determined following an efficient procedure:

- Step 1: the curve from points A to B and C to D was simulated by a varying quantity of fractal units I and II, respectively. The former was a curve with relatively flat slope, which can be fit by one piece fractal unit I (Figure 5). In point C, the porosity of the IFU was set equal to that presented in the PSD curve and thus 1765619 pieces of fractal unit II was required to achieve this purpose. Thereby, the PSD curve ranging from 10 nm to 357 000 nm was roughly simulated by fractal units I and II.

- Step 2: to improve the fitting degree around point E, 3569816 pieces of fractal unit III with pore size 266.667 nm, which equal the sub-pore size of fractal units II at 1th iteration, were supplemented to the IFU configuration.

Through step 1 and step 2, the whole PSD curve was nearly precisely simulated by the elementary IFU, as shown in Figure 5. However, the pore size less than 10 nm has not been examined in the MIP test for the limit mercury intrusion pressure, and consequently a porosity of 0.361 - 0.337 = 0.024 was excluded. Therefore, fractal unit IV was required to simulate the pore size distribution from point F to G.

- Step 3: the minimum pore size of fractal unit IV was set to be 0.2 nm, because Lloret and Villar (2007) considered that for compacted clays the pore size ranging between 0.2 and 2 nm can be identified as the intra-particle (inter-platelet) pore space. In order to achieve a strict correspondence to the calculated porosity $\phi = 0.361$, the amount of the fractal unit IV was therefore determined to be 3506993094.

4) Finally, the area of the filled surface can be calculated as:

$$S_{filled} = S_{IFU} - \sum_{j=1}^{IV} n_j S_j \tag{7}$$

where S_{filled} is the area of the filled surface, S_{IFU} is the total area of the integral IFU configuration,

n_j and S_j are the amount and area of each fractal unit, respectively.

The parameters of the IFU model are shown in Table 3 and relevant calculations can be referred to Equation (2) and Equation (3).

As shown in Figure 6, three basic Sierpinski type fractal units SA, SB-1 and SB-2, have been used to develop the fractal units I, II, III, IV and successively to built the IFU configuration. These basic fractal units can be converted into electrical equivalent circuits and the corresponding ETC can be calculated following the procedure mentioned in Section 3. The ETC of the integral IFU configuration can be calculated as:

$$k_{\text{eff}} = \frac{n_{\text{I}} S_{\text{I}} (k_{\text{SA}})_{i_{\text{I}}} + \frac{1}{2} \sum_{j=\text{II}}^{\text{IV}} n_j S_j (k_{\text{SB-1}} + k_{\text{SB-2}})_{i\,j}}{S_{\text{IFU}}} \tag{8}$$

where $(k_{\text{SA}})_{i_{\text{I}}}$ is the ETC of fractal unit I at its i^{th} iteration ($i = 5$ in the present case), and $(k_{\text{SB-1}} + k_{\text{SB-2}})_{i\,j}$ stands for the ETC of the j fractal unit (II, III, or IV) at their corresponding iteration i.

Table 3. The parameters of the IFU model.

FU	I	II	III	IV	Filled surface
Type	SA	SB-1 or SB-2	SB-1 or SB-2	SB-1 or SB-2	SB-1 or SB-2
$\lambda_{\max}$ (nm)	357000	800	266.667	5.4	—
Iteration	5	4	0	3	—
$\lambda_{\min}$ (nm)	1469.136	9.877	266.667	0.2	—
Area (nm^2)	1.147E12	5.76E6	6.402E5	262.44	1.019E13
Amount	1	1765619	3569816	3506993094	1

4.2 *Parameter calibration and model validation*

One of the involved parameter, k_{f} in Figure 4, was presumed to be related to the degree of water saturation, S_{r}, in the form of

$$k_{\text{f}} = k_{\text{a}} + S_{\text{r}}(k_{\text{w}} - k_{\text{a}}) = k_{\text{a}} + \frac{wG_{\text{s}}}{G_{\text{s}}/\rho_{\text{dry}} - 1}(k_{\text{w}} - k_{\text{a}}) \tag{9}$$

where, S_{r} is the degree of saturation, w is the water content, G_{s} is the specific gravity of solid phase, ρ_{dry} is the dry density, and $k_{\text{w}} = 0.60$ W/mK and $k_{\text{a}} = 0.026$ W/mK are the thermal conductivities of pore water and pore air at 20℃, respectively. Additionally, the measured thermal conductivity (0.851 W/mK) of series 3 in Table 1 was used to calibrate the other model parameter k_{s}, resulting in $k_{\text{s}} = 1.465$ W/mK. Equation (9) indicates that k_{f} increases with with dry density and water content, and thus resulting in the increase of k_{eff} (The relationship between k_{f} and k_{eff} can be referred to Figure 6).

To verify the proposed IFU model, the ETC of Series 1, 2, 4, 5 was calculated following the mentioned procedures and the results were obtained and compared to the measured ones in Figure 7. It can be observed from the results in Figure 7 that the calculated values are in good agreement with the experimental data, indicating the performance of the IFU model. It can also be found that the ETC of GMZ01 bentonite increases with dry density and water content, which is in accordance with the theoretical results. However, as shown in Equation (9), k_{f} was assumed to change linearly with degree of saturation, S_{r}, for all scales of pores. This is inconsistent with the real process of hydration during which the smaller pores achieve saturated state preferentially than the larger pores, i.e., the degree of saturation in different scales of pores are various. Additionally, the IFU configuration is developed according to the PSD curve which also significantly depends on dry density and water content. In other words, bentonite with different dry densities and water contents have different PSD curves, and therefore will result in different IFU configuration with different amounts and iterations of each type of FU (Table 3). These differences will also influence the value of k_{eff}, but can hardly be included in the present model. Therefore, further improvements are needed in the future work.

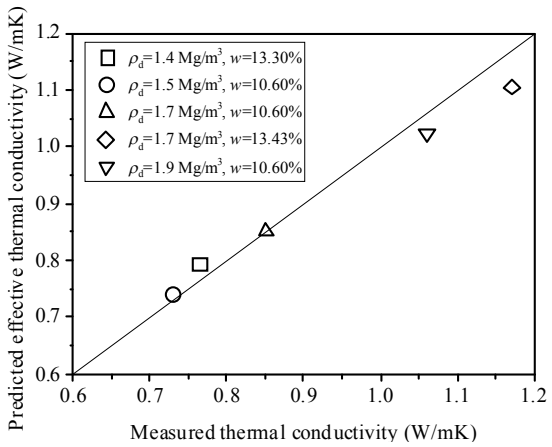

Figure 7. Comparisons between the predicted and measured thermal conductivity.

5 CONCLUSIONS

The pore size distribution curves of highly compacted bentonite are proved to be non-fractal, and thus can hardly be characterized by conventional fractal method. To address this non-fractal problem, the intermingled fractal units (IFU) theory was introduced to build a new model for predicting effective thermal conductivity (ETC) with consideration of the microstructure characteristics of GMZ01 bentonite. Firstly,

the IFU configuration was built with only three simple Sierpinski type fractal units following a more definite and imitable procedure according to the pore size distribution curves obtained from MIP test. Subsequently, the ETC of the IFU configuration was calculated via series-parallel electrical analogy equivalently converted from the IFU configuration. By comparing the predicted and measured results under different conditions, it is concluded that IFU model can reliably predict the ETC of GMZ01 bentonite which was largely governed by its dry density and water content. The tool developed here is helpful to further numerical modeling of the THM processes subjected by the GMZ01 bentonite.

6 ACKNOWLEDGEMENTS

The authors are grateful to the National Natural Science Foundation of China (Projects No. 41527801, 41672271).

7 REFERENCES

Atzeni, C., Pia, G. & Sanna, U. 2008. Fractal modelling of medium-high porosity SiC ceramics. *Journal of the European Ceramic Society* 28(14): 2809-2814.

Barry-Macaulay, D., Bouazza, A., Wang, B. & Singh, R.M. 2015. Evaluation of soil thermal conductivity models. *Canadian Geotechnical Journal* 52(11): 1892-1900.

Bartoli, F., Philippy, R., Doirisse, M., Niquet, S. & Dubuit, M. 2010. Structure and self-similarity in silty and sandy soils: the fractal approach. *European Journal of Soil Science* 42(2): 167-185.

Chen, B., Guo, J.X. & Zhang, H.X. 2016. Alteration of compacted GMZ bentonite by infiltration of alkaline solution. *Clay Minerals* 51(2): 237-247.

Chen, Y.F., Zhou, S., Hu, R. & Zhou, C.B. 2014. Estimating effective thermal conductivity of unsaturated bentonites with consideration of coupled thermo-hydro-mechanical effects. *International Journal of Heat and Mass Transfer* 72(3): 656-667.

Chen, Y.F., Wang, M., Zhou, S., Hu, R. & Zhou, C.B. 2015. An effective thermal conductivity model for unsaturated compacted bentonites with consideration of bimodal shape of pore size distribution. *Science China Technological Sciences* 58(2): 369-380.

Cho, W.J., Lee, J.O. & Kwon, S. 2011. An empirical model for the thermal conductivity of compacted bentonite and a bentonite-sand mixture. *Heat Mass Transfer* 47(11): 1385-1393.

Dong, Y., McCartney, J.S. & Lu, N. 2015. Critical review of thermal conductivity models for unsaturated soils. *Geotechnical and Geological Engineering* 33(2): 207-221.

Dueck, A. & Börgesson, L. 2015. Thermo-mechanically induced brittleness in compacted bentonite investigated by unconfined compression tests. *Engineering Geology* 193: 305-309.

Johnson, L.H ., Niemeyer, M., Klubertanz, G., Siegel, P. & Gribi, P. 2002. Calculations of the temperature evolution of a repository for spent fuel, vitrified high-level waste and intermediate level waste in Opalinus Clay. *Nagra Technical Report NTB 01-04*. Nagra, Wettingen, Switzerland.

Laine, H. & Karttunen, P. 2010. Long-term stability of bentonite - A Literature Review. *Working Report 2010-53*. POSIVA, Eurajoki, Finland.

Liu, Y., Cai, M. & Wang, J. 2007. Thermal properties of buffer material for high-level radioactive waste disposal. *Chinese Journal of Rock Mechanics and Engineering* 26(Supp2): 3891-3896. (In Chinese)

Lloret, A. & Villar, M.V. 2007. Advances on the knowledge of the thermo-hydro-mechanical behaviour of heavily compacted "FEBEX" bentonite. *Physics & Chemistry of the Earth Parts A/b/c*, 32(8-14): 701-715.

Mandelbrot, B.B. 1967. How long is the coast of Britain? Statistical self-similarity and fractional dimension. *Science* 156(3775): 636-638.

Perrier, E., Bird, N. & Rieu, M. 1999. Generalizing the fractal model of soil structure: the pore-solid fractal approach. *Geoderma* 88 (3-4): 137-164.

Pfeifer, P. & Avnir, D. 1983. Chemistry in noninteger dimensions between two and three, I. Fractal theory of heterogeneous surfaces. *Journal of Chemical Physics* 79(7): 3558-65.

Pia, G. & Sanna, U. 2013a. A geometrical fractal model for the porosity and thermal conductivity of insulating concrete. *Construction and Building Materials* 44(44): 551-556.

Pia, G. & Sanna, U. 2013b. Intermingled fractal units model and electrical equivalence fractal approach for prediction of thermal conductivity of porous materials. *Applied Thermal Engineering* 61(2): 186-192.

Pia, G. & Sanna, U. 2014a. An intermingled fractal units model to evaluate pore size distribution influence on thermal conductivity values in porous materials. *Applied Thermal Engineering* 65(1-2): 330-336.

Pia, G. & Sanna, U. 2014b. Case studies on the influence of microstructure voids on thermal conductivity in fractal porous media. *Case Studies in Thermal Engineering* 2: 8-13.

Pusch, R., Bluemling, P., & Johnson, L.H., 2003. Performance of strongly compressed MX-80 pellets under repository-like conditions. *Applied Clay Science* 23(1-4): 239-244.

Tang, A.M., Cui, Y.J. & Le, T.T. 2008. A study on the thermal conductivity of compacted bentonites. *Applied Clay Science* 41(3-4): 181-189.

Wan, M., Ye, W.M., Chen, Y.G., Cui, Y.J. & Wang, J. 2015. Influence of temperature on the water retention properties of compacted GMZ01 bentonite. *Environmental Earth Sciences* 73(8): 4053-4061.

Wen, Z.J. & Jintoku, T. 2005. Preliminary study on static mechanical property of GMZ Na-bentonite. *World Nuclear Geoscience* 22(4): 211-214. (In Chinese)

Wersin, P., Johnson, L.H. & McKinley, I.G. 2007. Performance of the bentonite barrier at temperatures beyond 100℃: a critical review. *Physics and Chemistry of the Earth* 32(8-14): 780-788.

Xu, Y.F., Sun, W.Y. & Wu, Z.G. 1997. On fractal structure of expansive soils in China. *Journal of Hohai University (Natural Sciences)* 25(1): 18-23.

Xu, Y.F. 2004. Calculation of unsaturated hydraulic conductivity using a fractal model for the pore-size distribution. *Computers and Geotechnics* 31(7): 549-557.

Ye, W.M., Wang, Q. & Pan, H. 2010. Thermal conductivity of compacted GMZ01 bentonite. *Chinese Journal of Geotechnical Engineering* 32(6): 821-826. (In Chinese)